A Humanized Monoclonal Antibody against the Enzymatic Subunit of Ricin Toxin Rescues Rhesus macaques from the Lethality of Aerosolized Ricin

Chad J. Roy[1,*], Dylan J. Ehrbar[2], Natasha Bohorova[3], Ognian Bohorov[3], Do Kim[3], Michael Pauly[3], Kevin Whaley[3], Yinghui Rong[2], Fernando J Torres-Velez[2], Ellen S Vitetta[4], Peter J. Didier[1], Lara Doyle-Meyers[1], Larry Zeitlin[3,*], and Nicholas J. Mantis[2,*]

[1]Tulane National Primate Research Center, Covington, Louisiana USA; [2]Division of Infectious Disease, Wadsworth Center, New York State Department of Health, Albany, NY 12208; [3]Mapp Biopharmaceutical, Inc. San Diego, CA 92121; [4]Departments of Immunology and Microbiology, University of Texas Southwestern Medical Center, Dallas, TX 75390

Running title: Rescue from ricin aerosol exposure

Keywords: MAb, ricin, toxin, biodefense, therapeutic

*Corresponding authors: Chad J. Roy, Tulane National Primate Research Center, Microbiology Division, 18703 Three Rivers Road, Covington, LA 70433; Tel 985-871-6417, email: croy@tulane.edu; *Larry Zeitlin, Mapp Biopharmaceutical, Inc. San Diego, CA 92121; Phone: 858-625-0335; email: larry.zeitlin@mappbio.com;*Nicholas Mantis, Division of Infectious Disease, Wadsworth Center, 120 New Scotland Avenue, Albany, NY 12208. Phone: 518-473-7487. email: nicholas.mantis@health.ny.gov

Abstract

Ricin toxin (RT) ranks at the top of the list of potential bioweapons of concern to civilian and military personnel alike due to its high potential for morbidity and mortality after inhalation. In non-human primates, aerosolized ricin triggers a severe acute respiratory distress characterized by perivascular and alveolar edema, neutrophilic infiltration, and severe necrotizing bronchiolitis and alveolitis. There are currently no approved countermeasures for ricin intoxication. In this report, we demonstrate the therapeutic potential of huPB10, a toxin-neutralizing humanized monoclonal antibody (MAb) against an immunodominant epitope on ricin's enzymatic A chain (RTA). Five rhesus macaques that received intravenous huPB10 (10 mg/kg) four hours after lethal dose ricin aerosol exposure all survived the toxin challenge, as compared to control animals, which succumbed to ricin intoxication within 30 h. Antibody treatment at 12 h after ricin exposure resulted in the survival of only one of five monkeys, indicating that, in the majority of animals, ricin intoxication and local tissue damage had progressed beyond the point where huPB10 intervention was beneficial. Change in pro-inflammatory cytokine/chemokines levels in bronchial alveolar lavage fluids before and after toxin challenge successfully clustered monkeys based on survival, as well as treatment group. IL-6 was the most apparent marker of ricin intoxication. This study represents the first demonstration in nonhuman primates that the lethal effects of inhalational ricin exposure can be negated by a drug candidate and opens up a path forward for product development.

53 .
54
55 **Introduction**

56 Ricin toxin (RT) is considered a high priority biothreat agent by the Centers for
57 Disease Control and Prevention (CDC), the US Department of Defense (DOD), and
58 NATO due to it's accessibility, stability, and high toxicity especially by the aerosol route.
59 (1, 2). In nonhuman primates (NHPs), inhalation of RT elicits the clinical equivalent of
60 acute respiratory distress syndrome (ARDS), characterized by widespread apoptosis of
61 alveolar macrophages, intra-alveolar edema, neutrophilic infiltration, accumulation of
62 pro-inflammatory cytokines, and fibrinous exudate (3, 4). Ricin also damages the lung
63 mucosa and triggers vascular leak due to direct damage to endothelial cells (5). Similar
64 effects are observed in mice, rats and swine (6-10). RT is derived from castor beans
65 (*Ricinus communis*) and is a 65 kDa heterodimeric glycoprotein consisting of two
66 subunits, RTA and RTB, joined via a single disulfide bond. RTB binds to glycoproteins
67 and glycolipids on mammalian cells and facilitates the retrograde transport of RT to the
68 endoplasmic reticulum (ER). In the ER, RTA is liberated from RTB and retrotranslocated
69 into the cytoplasm *via* the Sec61 complex (11). RTA is an RNA N-glycosidase that
70 catalyzes the hydrolysis of a conserved adenine residue within the sarcin/ricin loop of
71 28S rRNA, resulting in the inhibition of protein synthesis (12, 13) and the activation of
72 apoptosis (14). Alveolar macrophages are particularly sensitive to the cytotoxic effects
73 and secrete an array of pro-inflammatory cytokines before undergoing apoptosis (8, 9,
74 15).

75 In this report we investigated the potential of a humanized monoclonal antibody
76 (MAb) huPB10 to serve as a therapeutic in an established Rhesus macaques model of
77 RT inhalation (3, 16). PB10 was first described as a murine MAb with potent-toxin
78 neutralizing activity *in vitro* and *in vivo* (17). PB10 recognizes an immunodominant
79 epitope situated at the apex of RTA, relative to RTB (18, 19). Chimeric (cPB10) and fully
80 humanized (huPB10) versions of PB10 retain *in vitro* toxin-neutralizing activity and have
81 been shown to passively protect mice against lethal dose of RT administered by
82 injection or inhalation (20, 21). It was also demonstrated that huPB10 can rescue mice
83 from intoxication if administered 4-6 h after exposure (21). Based on these preliminary
84 findings, assessed the therapeutic potential of huPB10 in a well-established nonhuman

85 primate (NHP) model of ricin aerosol challenge (16). The NHP is believed to be the
86 model most representative of aerosolized exposure.
87
88 **Results**
89 A total of 12 rhesus macaques (~7 kg; range 3.8-10.2 kg) bred at Tulane National
90 Primate Research Center (TNPRC) were randomly assigned to three experimental
91 groups and then challenged with RT by small particle aerosol at a target dose of 18
92 µg/kg (**Table 1; Figure 1**). Animal studies were conducted in strict compliance with
93 protocols approved by TNPRC's Institutional Animal Care and Use Committee (IACUC).
94 Group 1 (n=2) received intravenous administration of saline 4 h post challenge. Animals
95 in groups 2 and 3 received huPB10 at 4 h or 12 h post challenge, respectively (**Table**
96 **1**). huPB10 was administered intravenously at a final dose of 10 mg/kg (**Table S1**). The
97 macaques were subjected to whole body plethysmography and radiotelemetry over the
98 course of the study. Animals surviving on day 14 post challenge were euthanized and
99 subjected to complete necropsy and histopathological analysis. Serum and bronchial
100 alveolar lavage (BAL) fluids were collected from the animals before and 24 h after
101 exposure to RT.
102 Control animals (n=2) succumbed to RT toxicosis within 36 hours of exposure.
103 (**Table 1; Figure 1**). The clinical progression of RT-induced intoxication of the control
104 animals was the same as in previous studies (3). Approximately 12-16 hours after
105 exposure, animals displayed reduced activity and fever (**Figure 2**). Clinical examination
106 conducted 24 h post exposure revealed respiratory complications, including bilateral
107 congestion and crackles, with dyspnea and tachypnea. Arterial oxygen ranged from 75-
108 85%. The clinical state of the animals continued to decline over the subsequent several
109 hours, manifested by a marked drop in normal activity and cyanotic mucous membrane.
110 In contrast, all five of the Rhesus macaques that received huPB10 at 4 h post-
111 ricin challenge time point survived (*P<0.01* compared to controls) and remained
112 otherwise normal for the duration of the three-week post-exposure observation period
113 (**Table 1: Figure 1**). Compared to the control animals, the five macaques in Group 2
114 presented with only minimal signs of distress: mild dyspnea, minimal tachypnea and

115 increased lung sounds upon physical examination at 24 h post-exposure. The animals
116 displayed no such symptoms upon physical examination on day 7.
117 Finally, only one of the five animals in Group 3 that received huPB10 at 12 h
118 survived RT challenge (**Table 1; Figure 1;** *P<0.01* and *P<0.05* compared to controls
119 and +4 h group, respectively). The remaining four animals succumbed to RT intoxication
120 between 44 and 72 h post challenge and followed a clinical course similar to the control
121 animals. HuPB10 was detected in the sera and BAL fluids collected at 24 h post RT
122 challenge, indicating that biodistribution of huPB10 was similar between groups 2 and 3.
123 Gross examination of the lungs from sham-treated control animals showed
124 coalescing hemorrhage with frothy exudate marked by fibrin in lung parenchyma
125 (**Figure S1**). The lungs of control animals were grossly described as fibrinosuppurative
126 bronchointerstitial pneumonia with pulmonary edema and bronchial epithelial necrosis,
127 with severe fibrinosuppurative lymphadenitis in the bronchial lymph nodes. The wet
128 weights of control animal lungs were >150 grams in contrast to a normal wet lung
129 weight of ~30-40 grams in naïve animals of approximately the same body weight.
130 Histologically, the lungs of sham-treated animals showed hallmark inflammation
131 consistent with RT-induced injury, characterized by marked edema, corresponding
132 hemorrhage, and numerous infiltrates. The pathological outcome of the four animals in
133 Animals in Group 3 that succumbed to RT intoxication resembled the control animals.
134 There was extensive pulmonary congestion, edema, inflammation with infiltrates, and
135 punctate hemorrhage evident. Gross lung weights were similar to RT-challenged control
136 animals (>140 g) with clear signs of hemorrhage.
137 Pathological analysis of the lung tissues collected at the time of euthanasia (day 21
138 post challenge) from the five survivors in Group 2 that had been treated with huPB10 at
139 4 h and the single animal in Group 3 (DR61) revealed evidence of chronic inflammation
140 and a distinctive fibrosis proximal to the respiratory bronicholes, reminiscent of past
141 studies in which animals had received sub-lethal exposures to RT (22).
142 Sera and BAL fluids collected before (day -7) and 24 h post RT challenge were
143 subjected to analysis with a 29-plex cytokine/chemokine/growth factor Luminex array as
144 a means to assess the impact of huPB10 on local and systemic inflammatory
145 responses. In the sera of the two control animals, there were 12 cytokines/chemokines

146 that were significantly different in serum post- versus pre-challenge; 11 cytokines were
147 increased, while one (IL-8) was decreased (**Figure 3A; S2**). Most notable were IL-6
148 (~500-fold increase) and IL-1RA (~256-fold increase). VEGF was also elevated,
149 possibly reflecting response to pulmonary insult. Analysis of sera from animals that
150 received huPB10 at 4 h post challenge indicated that only four cytokine/chemokines
151 were significantly different from pre-challenge levels (3 up;1 down), including a ~4-fold
152 increase in IL-6. IL-1RA and VEGF levels were unchanged. In animals that received
153 huPB10 at 12 h after RT challenge, a total of six cytokines/chemokines changed relative
154 to pre-challenge levels, although the magnitude of these changes was lower than that if
155 the control animals, possibly reflecting a dampening of the inflammatory response as a
156 consequence of huPB10 intervention. Principle component analysis (PCA) of fold-
157 change in cytokine/chemokine levels from serum samples from all 12 monkeys did not
158 reveal any clustering by experimental group or survival (**Figure S3A-C**), signifying that
159 serum inflammatory responses are not indicative of experimental outcome.
160 The impact of huPB10 intervention was much more apparent in BAL fluids than in
161 sera (**Figure 3B**). Within group 2, a total of 21 cytokines/chemokines were significantly
162 elevated following RT challenge (as compared to pre-challenge levels), with IL-6 being
163 the most pronounced. In group 3, there were 25 cytokines/chemokines that were
164 significantly elevated compared to pre-challenge levels. Seven cytokines/chemokines
165 differed between the groups 2 and 3 with the most notable being IL-6, which was 32-fold
166 elevated in group 2 and 181-fold elevated in group 3. PCA successfully clustered
167 animals by both group and survival status, demonstrating that the localized cytokine
168 responses in the BAL are more closely related to survival than the systemic responses
169 (**Figure S3D-E**). The relative contributions of the different cytokines/chemokines
170 responsible for segregating the animals into clusters are shown in **Figure S3F**.
171

172 **Discussion**

173 The results of this study constitute a significant advance in longstanding efforts to
174 develop effective medical countermeasures against RT inhalation (2, 23). Foremost, it is
175 the first demonstration in NHPs that a MAb can rescue animals from the lethal effects of
176 aerosolized ricin toxin exposure. Studies in primates are important because anti-RT

177 products for humans must adhere to the Food and Drug Administration's (FDA) Animal
178 Rule; human challenge studies with RT are obviously unethical. The well-established
179 model of aerosolized RT challenge in Rhesus macaques was a prerequisite for the
180 therapeutic study conducted herein (3, 16, 24). Comparative models in mice (6, 8, 25)
181 and swine (10) may also be important for therapeutic development under Animal Rule
182 guidelines. The fact that all five animals in group 2 (+4 h huPB10 intervention), and one
183 animal in group 3 (+12 h huPB10 intervention), survived exposure to RT indicates that a
184 significant proportion of RT remains accessible to huPB0 in the alveolar space and/or
185 interstitial fluids for hours after inhalational exposure. This finding is consistent with
186 reports in mice with huPB10 and other anti-RT MAbs (6, 7, 21, 26), but surprising all
187 the same considering the extraordinary sensitivity of the lung mucosa to the effects of
188 toxin exposure (27).
189 We postulate that high dose intravenous delivery of huPB10 results in the
190 accumulation of huPB10 within the lung mucosa and alveolar space where it can
191 engage free (soluble) or receptor-bound RT. Indeed, IV administration of recombinant
192 anti-viral IgG1 MAbs results a corresponding linear distribution of antibodies lung (28,
193 29). Whether transudation or active transport of serum antibodies into the lung mucosa
194 is triggered by RT exposure has not been evaluated. Nonetheless, once in the lung
195 mucosa, huPB10 presumably limits toxin uptake into target cells (e.g., macrophages
196 and airway epithelial cells) and/or interferes with ricin intracellular transport in the event
197 that endocytosis of RT-antibody complexes should occur (30, 31). Work by Magun and
198 colleagues made it clear more than a decade ago that protecting alveolar macrophages
199 is paramount in limiting toxin-induced lung damage (9, 32).
200 It is worth underscoring the value of the 29-plex monkey cytokine/chemokine/growth
201 factor array in not only identifying local inflammatory markers like IL-6 that arise
202 following RT exposure but also enabling through PCA the unbiased clustering of
203 specific animals based on survival or experimental group. Identifying an inflammatory
204 “fingerprint” associated with RT exposure has obvious applications in diagnostics,
205 especially in the context of biodefense where early clinical symptoms following
206 exposure to different toxins and pathogens may in fact be indistinguishable (33). As
207 noted above, IL-6 levels were particularly elevated following RT exposure, which is

208 consistent with what has been observed in mice (34). IL-6 is a particularly potent driver
209 of pulmonary inflammation and could very well be a major contributor to RT-induced
210 pathology in conjunction with RT's other properties, including agglutinin activity and the
211 capacity to induce vascular leak syndrome (5, 35). We recently reported that human
212 lung epithelial cell lines preferentially secrete IL-6 following RT exposure, especially in
213 the presence of pro-apoptotic factors like TRAIL (36). It has been suggested that anti-
214 inflammatory agents may extend the therapeutic window of anti-RT MAbs by
215 suppressing bystander tissue damage (26). Whether such directed immunotherapies
216 would have utility in the context of potent toxin-neutralizing antibody like huPb10
217 remains to be seen. At least early intervention with huPB10 was sufficient to render RT
218 effectively inert within the context of the lung and it seems unlikely that supplementing
219 treatment with anti-inflammatory agents would afford much additional benefit.
220
221 **Methods**
222 **Ricin toxin and huPB10.** Purified ricin toxin derived from castor beans (*Ricinus*
223 *communis*) was produced as previously described (37). HuPB10 was expressed using a
224 *Nicotiana benthamiana*-based manufacturing platform. The properties of huPB10 used
225 in this study are shown in **Table S1.**
226
227 **Animal care and use.** Rhesus macaques were born and housed at the Tulane
228 National Primate Research Center (Covington, LA), which is US Department of
229 Agriculture-licensed and fully accredited by the Association for Assessment and
230 Accreditation of Laboratory Animal Care (AAALAC). Aerosolization, dosing and delivery
231 of RT were performed as described (16). The LD_{50} of ricin is 5.8 μg/kg body weight and
232 the target dose for this experiment was set at the equivalent of three LD_{50}s (≈18 μg/kg).
233 The mean inhaled dose of ricin across all animals was 4.4 ± 1.4 LD_{50}s. At 4 h or 12
234 hours post-exposure, designated animal groups received a single intravenous
235 administration of huPB10 by slow infusion at an individualized unit dose of 10 mg/kg.
236 Sham-treated animals received saline at the 4h time point. Treated animals were
237 observed for signs of adverse reactions to the MAb during administration and
238 throughout the anesthesia recovery period. Animals were bled just before and 24 h

239 following aerosol challenge. Blood was also collected when the animals either
240 succumbed to intoxication or 21 d after challenge, when the experiment was terminated.
241 Animals determined to be in respiratory distress and those that survived for 21 d after
242 exposure to ricin were euthanized by an overdose of sodium pentobarbital, consistent
243 with the recommendation of the American Veterinary Medical Association's Panel on
244 Euthanasia, and submitted for necropsy. All methods were approved by the Tulane
245 University's IACUC. After gross necropsy, tissues were collected in neutral buffered
246 zinc-formalin solution (Z-Fix Concentrate, Anatach). Tissues were processed,
247 sectioned, and stained as previously described (3).
248
249 **Statistics**. Statistical analysis was carried out with GraphPad Prism 6 (GraphPad
250 Software, La Jolla California USA). The difference in outcomes between groups was
251 determined by Fisher's exact test (two-tailed) and the mean survival times after
252 exposure to RT were compared by log-rank analysis of Kaplan–Meier survival curves.
253 The statistical significance of the effects of ricin challenge and huPB10 intervention on
254 cytokine levels were analyzed with two-way repeated measures ANOVAs in both serum
255 and BAL, with the repeated measures being pre- and post-exposure status, and
256 treatment group as the independent measure. Resulting p-values were corrected with
257 the Benjamini, Krieger, and Yekutieli method to control false discovery rate. All
258 analyses were performed on $\log^2$ transformed raw fluorescent intensity values to avoid
259 the need to censor values. PCA analysis was performed using singular value
260 decomposition with the R package FactoMineR (38). Heatmap construction using raw
261 fold change values was done using GraphPad Prism 6. Hierarchical clustering and
262 scaled heatmap construction was completed with the R package pheatmap (39).
263
264 **Author contributions.** NB, OB, DK, MP, KW and ESV generated reagents; PJD, LDM,
265 YR, and CJR conducted animal studies and animal tissue/sample analysis; DJE
266 performed statistical analysis; CJR, NJM, and LZ are responsible for experimental
267 design and CJR, NM and ESV prepared the manuscript.
268

Conflicts of interest. NB, OB, DK, MP are Mapp Biopharmaceutical employees and shareholders. KW and LZ are employees, shareholders, and co-owners of Mapp Biopharmaceutical. The remaining authors declare no conflicts of interest.

Acknowledgements. This work was supported by R01AI098774 to LZ and Contract No. HHSN272201400021C to NJM from the National Institutes of Allergy and Infectious Diseases, National Institutes of Health (NIH), as well as the National Center for Research Resources and the Office of Research Infrastructure Programs (ORIP) of the NIH through grant OD011104 at the Tulane National Primate Research Center to CJR. The content is solely the responsibility of the authors and does not necessarily represent the official views of the National Institutes of Health. The funders had no role in study design, data collection and analysis, decision to publish, or preparation of the manuscript.

References

1. Cieslak TJ, Kortepeter MG, Wojtyk RJ, Jansen HJ, Reyes RA, Smith JO, et al. Beyond the Dirty Dozen: A Proposed Methodology for Assessing Future Bioweapon Threats. *Mil Med.* 2018;183(1-2):e59-e65.
2. Wolfe DN, Florence W, and Bryant P. Current biodefense vaccine programs and challenges. *Human vaccines & immunotherapeutics.* 2013;9(7):1591-7.
3. Pincus SH, Bhaskaran M, Brey RN, 3rd, Didier PJ, Doyle-Meyers LA, and Roy CJ. Clinical and Pathological Findings Associated with Aerosol Exposure of Macaques to Ricin Toxin. *Toxins (Basel).* 2015;7(6):2121-33.
4. Wilhelmsen CL, and Pitt ML. Lesions of acute inhaled lethal ricin intoxication in rhesus monkeys. *Vet Pathol.* 1996;33(3):296-302.
5. Soler-Rodriguez AM, Ghetie MA, Oppenheimer-Marks N, Uhr JW, and Vitetta ES. Ricin A-chain and ricin A-chain immunotoxins rapidly damage human endothelial cells: implications for vascular leak syndrome. *Exp Cell Res.* 1993;206(2):227-34.
6. Poli MA, Rivera VR, Pitt ML, and Vogel P. Aerosolized specific antibody protects mice from lung injury associated with aerosolized ricin exposure. *Toxicon.* 1996;34(9):1037-44.

300 7. Pratt TS, Pincus SH, Hale ML, Moreira AL, Roy CJ, and Tchou-Wong KM.
301 Oropharyngeal aspiration of ricin as a lung challenge model for evaluation of the
302 therapeutic index of antibodies against ricin A-chain for post-exposure treatment. *Exp*
303 *Lung Res.* 2007;33(8-9):459-81.
304 8. Wong J, Korcheva V, Jacoby DB, and Magun B. Intrapulmonary delivery of ricin at
305 high dosage triggers a systemic inflammatory response and glomerular damage. *Am*
306 *J Pathol.* 2007;170(5):1497-510.
307 9. Lindauer ML, Wong J, Iwakura Y, and Magun BE. Pulmonary inflammation triggered
308 by ricin toxin requires macrophages and IL-1 signaling. *J Immunol.*
309 2009;183(2):1419-26.
310 10. Katalan S, Falach R, Rosner A, Goldvaser M, Brosh-Nissimov T, Dvir A, et al. A
311 novel swine model of ricin-induced acute respiratory distress syndrome. *Dis Model*
312 *Mech.* 2017;10(2):173-83.
313 11. Spooner RA, and Lord JM. How Ricin and Shiga Toxin Reach the Cytosol of
314 Target Cells: Retrotranslocation from the Endoplasmic Reticulum. *Curr Top Microbiol*
315 *Immunol.* 2012;357:19-40.
316 12. Endo Y, Mitsui K, Motizuki M, and Tsurugi K. The mechanism of action of ricin
317 and related toxic lectins on eukaryotic ribosomes. The site and the characteristics of
318 the modification in 28 S ribosomal RNA caused by the toxins. *J Biol Chem.*
319 1987;262(12):5908-12.
320 13. Endo Y, and Tsurugi K. RNA N-glycosidase activity of ricin A-chain. Mechanism
321 of action of the toxic lectin ricin on eukaryotic ribosomes. *J Biol Chem.*
322 1987;262(17):8128-30.
323 14. Tesh VL. The induction of apoptosis by Shiga toxins and ricin. *Curr Top Microbiol*
324 *Immunol.* 2012;357:137-78.
325 15. Brown RF, and White DE. Ultrastructure of rat lung following inhalation of ricin
326 aerosol. *Int J Exp Pathol.* 1997;78(4):267-76.
327 16. Roy CJ, Brey RN, Mantis NJ, Mapes K, Pop IV, Pop LM, et al. Thermostable ricin
328 vaccine protects rhesus macaques against aerosolized ricin: Epitope-specific
329 neutralizing antibodies correlate with protection. *Proc Natl Acad Sci U S A.*
330 2015;112(12):3782-7.

331 17. O'Hara JM, Neal LM, McCarthy EA, Kasten-Jolly JA, Brey RN, 3rd, and Mantis
332 NJ. Folding domains within the ricin toxin A subunit as targets of protective
333 antibodies. *Vaccine.* 2010;28:7035-46.
334 18. Toth Rt, Angalakurthi SK, Van Slyke G, Vance DJ, Hickey JM, Joshi SB, et al.
335 High-Definition Mapping of Four Spatially Distinct Neutralizing Epitope Clusters on
336 RiVax, a Candidate Ricin Toxin Subunit Vaccine. *Clin Vaccine Immunol.* 2017.
337 19. Vance DJ, and Mantis NJ. Resolution of two overlapping neutralizing B cell
338 epitopes within a solvent exposed, immunodominant alpha-helix in ricin toxin's
339 enzymatic subunit. *Toxicon.* 2012;60(5):874-7.
340 20. Sully EK, Whaley K, Bohorova N, Bohorov O, Goodman C, Kim D, et al. A
341 tripartite cocktail of chimeric monoclonal antibodies passively protects mice against
342 ricin, staphylococcal enterotoxin B and Clostridium perfringens epsilon toxin. *Toxicon.*
343 2014;92:36-41.
344 21. Van Slyke G, Sully EK, Bohorova N, Bohorov O, Kim D, Pauly MH, et al.
345 Humanized Monoclonal Antibody That Passively Protects Mice against Systemic and
346 Intranasal Ricin Toxin Challenge. *Clin Vaccine Immunol.* 2016;23(9):795-9.
347 22. Bhaskaran M, Didier PJ, Sivasubramani SK, Doyle LA, Holley J, and Roy CJ.
348 Pathology of lethal and sublethal doses of aerosolized ricin in rhesus macaques.
349 *Toxicol Pathol.* 2014;42(3):573-81.
350 23. Reisler RB, and Smith LA. The need for continued development of ricin
351 countermeasures. *Adv Prev Med.* 2012;2012:149737.
352 24. Roy CJ, Song K, Sivasubramani SK, Gardner DJ, and Pincus SH. Animal Models
353 of Ricin Toxicosis. *Curr Top Microbiol Immunol.* 2012.
354 25. Wong J, Korcheva V, Jacoby DB, and Magun BE. Proinflammatory responses of
355 human airway cells to ricin involve stress-activated protein kinases and NF-kappaB.
356 *Am J Physiol Lung Cell Mol Physiol.* 2007;293(6):L1385-94.
357 26. Gal Y, Mazor O, Falach R, Sapoznikov A, Kronman C, and Sabo T. Treatments
358 for Pulmonary Ricin Intoxication: Current Aspects and Future Prospects. *Toxins*
359 *(Basel).* 2017;9(10).

360 27. van Deurs B, Hansen SH, Petersen OW, Melby EL, and Sandvig K. Endocytosis,
361 intracellular transport and transcytosis of the toxic protein ricin by a polarized
362 epithelium. *EurJCell Biol.* 1990;51(1):96-109.
363 28. Dall'Acqua WF, Kiener PA, and Wu H. Properties of human IgG1s engineered for
364 enhanced binding to the neonatal Fc receptor (FcRn). *J Biol Chem.*
365 2006;281(33):23514-24.
366 29. Wu H, Pfarr DS, Johnson S, Brewah YA, Woods RM, Patel NK, et al.
367 Development of motavizumab, an ultra-potent antibody for the prevention of
368 respiratory syncytial virus infection in the upper and lower respiratory tract. *J Mol Biol.*
369 2007;368(3):652-65.
370 30. O'Hara JM, and Mantis NJ. Neutralizing monoclonal antibodies against ricin's
371 enzymatic subunit interfere with protein disulfide isomerase-mediated reduction of
372 ricin holotoxin in vitro. *J Immunol Methods.* 2013;395(1-2):71-8.
373 31. Yermakova A, Klokk TI, O'Hara JM, Cole R, Sandvig K, and Mantis NJ.
374 Neutralizing Monoclonal Antibodies against Disparate Epitopes on Ricin Toxin's
375 Enzymatic Subunit Interfere with Intracellular Toxin Transport. *Sci Rep.*
376 2016;6:22721.
377 32. Wong J, Magun BE, and Wood LJ. Lung inflammation caused by inhaled
378 toxicants: a review. *Int J Chron Obstruct Pulmon Dis.* 2016;11:1391-401.
379 33. Lipscomb MF, Hutt J, Lovchik J, Wu T, and Lyons CR. The pathogenesis of
380 acute pulmonary viral and bacterial infections: investigations in animal models. *Annu*
381 *Rev Pathol.* 2010;5:223-52.
382 34. Sabo T, Gal Y, Elhanany E, Sapoznikov A, Falach R, Mazor O, et al. Antibody
383 treatment against pulmonary exposure to abrin confers significantly higher levels of
384 protection than treatment against ricin intoxication. *Toxicol Lett.* 2015;237(2):72-8.
385 35. Rubini A. Interleukin-6 and lung inflammation: evidence for a causative role in
386 inducing respiratory system resistance increments. *Inflamm Allergy Drug Targets.*
387 2013;12(5):315-21.
388 36. Rong Y, Westfall J, Ehrbar D, LaRocca T, and Mantis N. TRAIL (CD253)
389 Sensitizes Human Airway Epithelial Cells to Toxin-Induced Cell Death. *bioRxiv.* 2018.

390 37. Smallshaw JE, Firan A, Fulmer JR, Ruback SL, Ghetie V, and Vitetta ES. A novel
391 recombinant vaccine which protects mice against ricin intoxication. *Vaccine.*
392 2002;20(27-28):3422-7.
393 38. Lê S, Josse J, and Husson F. FactoMineR: An R Package for Multivariate
394 Analysis. *Journal of Statistical Software.* 2008;25(1):1-18.
395 39. Kolde R. pheatmap: Pretty Heatmaps. https://cran.r-
396 project.org/web/packages/pheatmap/index.html. Updated 2018-05-19.
397
398

399 **Figure Legends**

400 **Figure 1. Effect of huPB10 on the survival of animals exposed to aerosolized**
401 **RT** A. Animals were exposed to aerosolized RT aerosol and the individual RT doses ,
402 expressed in µg/kg inhaled, and clustered by treatment group, show minimal variation in
403 dosing, bars represent group mean ± standard deviation; the aerosol target dose of 18
404 µg/kg represented by segmented line. B. Macaque survival is represented by survival
405 curve. The two control animals succumbed to intoxication by day 2; treatment with
406 huPB10 at 4 h post ricin challenge resulted in 5/5 survival, while treatment with huPB10
407 at 12 h resulted in only 1/5 survivors.

408

409 **Figure 2. Physiological response to RT.** A. Radiotelemetry of core temperature of
410 rhesus macaques treated with huPB10 either at 4 h or 12 h post-exposure to
411 aerosolized RT. Continuous monitoring showed significant differences ($P<0.005$)
412 between the initiation and tempo of pyrexia that was dependent on the time to treat. B.
413 Fever intensity showed differences between the relative change (increase) based upon
414 time to treat. Respiratory function measured by whole-body
415 plethysmography. Respiratory function was measured *via* head-out conductance
416 plethysmography prior to and at timed intervals post challenge. C. Significant changes
417 ($P<0.05$) in post-exposure group tidal volume was observed among animals rescued
418 from ricin intoxication, (D) although compensatory changes in frequency resulted in
419 minimal observable changes in minute volume, with some animals producing increased
420 minute volumes +24 h post-exposure to ricin.

421

422 **Figure 3. Cytokine profiles of serum and BAL in RT challenged Rhesus**
423 **macaques.** Heatmaps present log_2-fold change of cytokines in (A) sera and (B) BALs,
424 comparing samples collected 24 hours post-challenge to those collected 7 days pre-
425 challenge. Animals are separated into groups for controls, 4-hour, and 12-hour huPB10
426 interventions. Increases in cytokine levels are shown in red, while decreases are shown
427 in blue. Specific values for the fold changes are shown within each cell and based on
428 single 29-plex analysis. A subset of cytokine changes were confirmed using BD™ CBA
429 Human Inflammatory Cytokines Kit.

430 **Tables**

431

Table 1. Experimental groups and outcome of ricin challenge

					huPB10 (μg/ml)[c]			
Group	**ID**	**kg**	**M/F[a]**	**RT[b]**	**serum**	**BAL**	**TTD[d]**	**#/total**
Control	DH27	9.7	M	14	-	-	28 h	
	JP56	8.4	M	26	-	-	30 h	0/2
+4 h huPB10	LJ80	4.4	M	31	157	2.8	+	
	LB98	4.9	M	29	177	2.7	+	
	EM61	9.5	M	31	207	2.5	+	
	IC70	5.9	F	26	225	3.6	+	
	IL40	6.1	F	33	147	3.2	+	5/5
+12 h huPB10	JM39	9.4	M	22	205	42.8	72 h	
	DR61	10.2	F	24	265	3.9	+	
	KP48	5.8	M	30	203	25.7	48 h	
	KR49	5.7	M	29	151	3.1	49 h	
	LB26	3.8	M	29	191	11.3	44 h	1/5

[a], sex of animal; [b], ricin toxin (RT) dose (μg/kg) received per animal; [c], huPB10 in serum and BAL from samples collected at 24 h post challenge. The average in serum was 182.6 μg/ml and 203 μg/ml for the +4 and +12 h groups, respectively. In the BAL, the was 3.04 μg/ml and 17.3 μg/ml, respectively. Times of huPB10 administration are approximate (~ 30 minutes of point estimate); the logistics of performing slow intravenous infusion of huPB10 in monkeys initiated and was times at 4 hours from each of the individual ricin aerosol challenge events and was performed in sequence; [d], time to death (TTD); +, indicates survival for 21 day duration of study.

432

433

434 **Supplemental Material**

435

436 Supplemental Methods

437

438 **Animal Husbandry and Telemetry.** Rhesus macaques were born and housed at the
439 Tulane National Primate Research Center (Covington, LA), which is US Department of
440 Agriculture-licensed and fully accredited by the Association for Assessment and
441 Accreditation of Laboratory Animal Care. Subcutaneous radiotelemetry transmitters
442 combined with sensors capable of detecting biopotential signals of an electrocardiogram
443 as well as thermistor-type sensors capable of detecting temperature signals (T34G-8;
444 Konigsberg Instruments) were surgically implanted under aseptic conditions in 8 of the
445 12 vaccinated macaques and both control macaques before the start of the study.
446 Animals determined to be in respiratory distress and those that survived for 21 d after
447 exposure to ricin were euthanized by an overdose of sodium pentobarbital, consistent
448 with the recommendation of the American Veterinary Medical Association's Panel on
449 Euthanasia, and submitted for necropsy. All methods were approved by the Tulane
450 Institutional Animal Care and Use Committee (IACUC).

451

452 **Treatment of Rhesus macaques**. At 4 h or 12 hours postexposure, designated animal
453 groups received a single intravenous administration of huPB10 by slow infusion at an
454 individualized unit dose of 10 mg/kg. Sham-treated animals were administered saline for
455 injection at the four-hour time point. Treated animals were observed for signs of
456 adverse reactions to the antibody during administration and throughout anesthesia
457 recovery period. Animals were bled just before and 24 h following aerosol challenge.
458 Blood was also collected when the animals either succumbed to intoxication or 21 d
459 after challenge, when the experiment was terminated.

460

461 **RT aerosolization, dosing, and calculation**. Aerosolization, dosing and delivery of
462 ricin were performed as described (16). Inductive plethysmography that measures
463 volume of air breathed by each individual animal per minute was performed just before
464 the ricin exposure. Ricin was dissolved in 10 mL sterile phosphate buffer saline to the

465 desired concentration for each animal based on plethysmography data obtained 2 d
466 before the exposure. Aerosols were generated directly into a head-only chamber using
467 a Collision three jet-nebulizer (BGI) with fully automated management control system
468 (Biaera Technologies, Hagerstown, MD) all within a Class III biological safety cabinet
469 housed within the TNPRC high-containment (BSL-3) laboratories. The nebulizer
470 operated at 18 lb/inch^2 equating to a flow of 7.5 L/min and produced 3.0E+04 particles
471 per cc with a mass median aerodynamic diameter of ~1.4 μm. Each discrete aerosol
472 exposure lasted 10 minutes (per animal). Air samples were continuously obtained
473 during the exposure and the protein concentrations of these samples were determined
474 using a micro-BSA protein assay kit (Thermo Scientific). The aerosol concentrations
475 were determined and the inhaled dose of RT for each animal was calculated by
476 multiplying the empirically determined aerosol exposure concentration (μg/liter of air) in
477 the chamber by volume of air estimated to have been breathed by the animal (via
478 results of plethysmography just before exposure). The LD_{50} of ricin is 5.8 μg/kg body
479 weight and the target dose for this experiment was set at the equivalent of three LD_{50}s
480 (≈18 μg/kg). The mean inhaled dose of ricin across all animals was 4.4 ± 1.4 LD_{50}s.
481
482 **Statistics**. Statistical analysis was carried out with GraphPad Prism 6 (GraphPad
483 Software, La Jolla California USA). The difference in outcomes between groups was
484 determined by Fisher's exact test (two-tailed) and the mean survival times after
485 exposure to ricin were compared by log-rank analysis of Kaplan–Meier survival curves.
486 The statistical significance of the effects of ricin challenge and huPB10 intervention on
487 cytokine levels were analyzed with two-way repeated measures ANOVAs in both serum
488 and BAL, with the repeated measures being pre- and post-exposure status, and
489 treatment group as the independent measure. Resulting p-values were corrected with
490 the Benjamini, Krieger, and Yekutieli method to control false discovery rate. All
491 analyses were performed on log^2 transformed raw fluorescent intensity values to avoid
492 the need to censor values. PCA analysis was performed using singular value
493 decomposition with the R package FactoMineR (38). Heatmap construction using raw
494 fold change values was done using GraphPad Prism 6. Hierarchical clustering and
495 scaled heatmap construction was completed with the R package pheatmap (39).

496

497 **Tissue Collection, Histological Analysis, and Special Stains**. After gross necropsy,
498 tissues were collected in neutral buffered zinc-formalin solution (Z-Fix Concentrate,
499 Anatach). Tissues were processed, sectioned, and stained as previously described (3).

500

501 **Supplemental Table**
502

Table S1. Characteristics of huPB10 used in study

Test Parameters	Test Method	Result
Concentration	UV Absorbance	19.7 mg/mL
Appearance	Visible	clear, liquid
Physical/chemical	pH Determination	5.6
Purity	SDS-PAGE	> 99%
Osmolality	Micro-Osmometer	412 mOS/kg
Bioburden	Bioburden Testing	0 CFU/mL
Aggregates	Size Exclusion HPLC	1.90%
Potency	ELISA	20.0 mg/mL
Safety	Endotoxin	0.2 EU/mg

503

504

505

506

507 **Figure S1. Gross pathology associated with RT exposure and huPB10**
508 **intervention**. The lungs of sham-treated animals (Figure 3a) show hallmark
509 inflammation, marked edema, corresponding hemorrhage, and numerous infiltrates;
510 grossly, wet weight at 3x normal with coalescing hemorrhage. Animals treated with
511 huPB10 at 4 h (Figure 3b & 3c) show remarkably little pulmonary damage, with
512 occasional infiltrates; lung wet weights were essentially normal. Animals treated with
513 huPB10 at 12 hours (Figure 3d) demonstrated mild to moderate inflammation with
514 infiltrates, edema, and punctate hemorrhage evident; gross lung weight were
515 approximately 2x with clear signs of hemorrhage. Original magnification at 10x
516

517 **Fig. S2 Scaled heatmap and cluster analysis of log2-fold changes in cytokine**
518 **levels in individual macaques following ricin challenge.** Heatmaps visualizing log2-
519 fold changes in cytokines in serum (A) and BAL (B). Both individual animals and
520 cytokines are arranged by hierarchical clustering, represented by dendrograms on top
521 and to the right of the heatmaps, respectively. Surviving animals are marked in white in
522 the top bar above the heatmap, while dead animals are in black. In the bar below this,
523 the 4-hour group of animals are marked in red, the 12-hour group in blue, and the
524 control group in green. Fold change values are centered and scaled for each cytokine
525 by first subtracting the mean fold change from each value and then dividing by the
526 standard deviation of that cytokine.
527

528 **Fig. S3 Principal component analysis of cytokine fold changes following RT**
529 **challenge.** Scatter plots of first 2 principal components of log2-transformed cytokine
530 fold changes in A-C) BAL and (D-F) serum from all animals included in the study,
531 calculated used singular value decomposition. Each dot represents an individual
532 monkey; red for those in the 4-hour group, black for the 12-hour group, and green for
533 the control group. 95% confidence ellipses of the group means are represented in the
534 color of the group they correspond to. Eigenvectors for (C) BAL and (F) and analyses
535 are colored to show the percent contribution of each variable to the principal
536 components.

Figure 1

A.

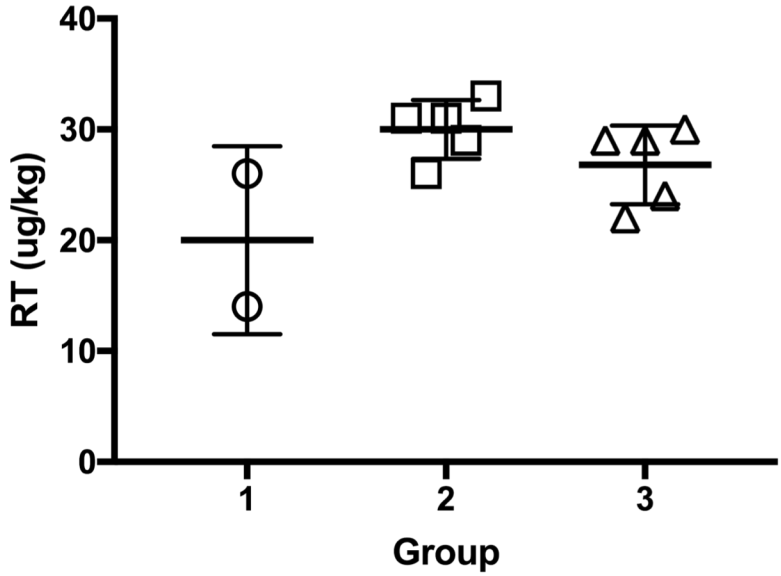
40
30
20
10
0
RT (ug/kg)
1
2
3
Group

B.

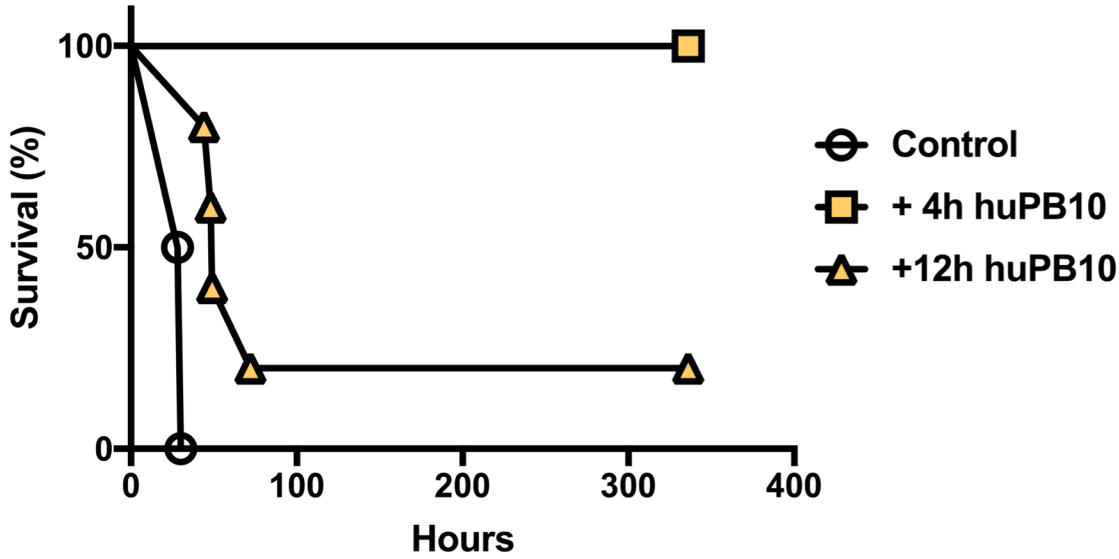
100
50
0
Survival (%)
0
100
200
300
400
Hours
Control
+ 4h huPB10
+12h huPB10

Figure 2

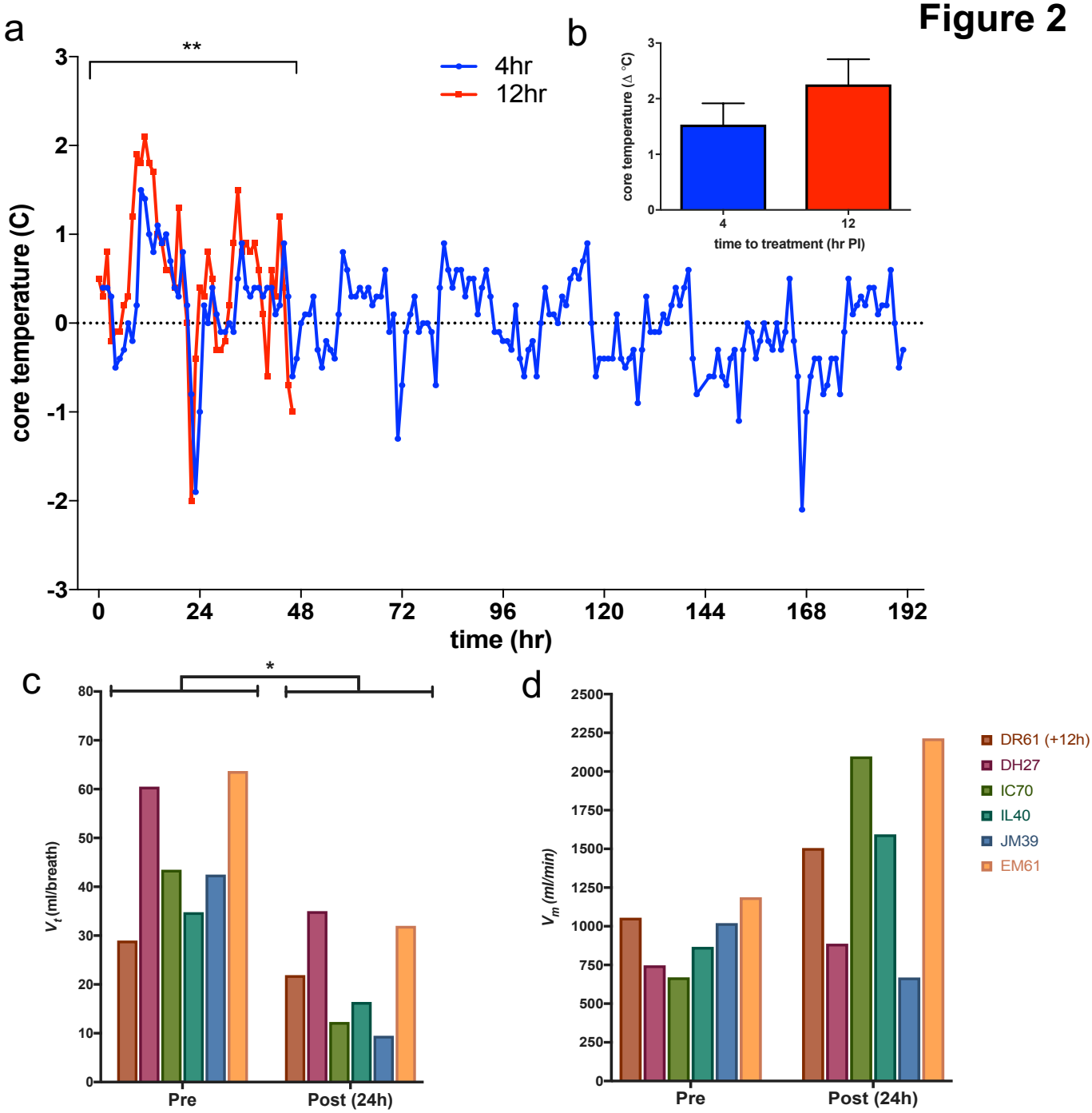
a
**
4hr
12hr
core temperature (C)
time (hr)
b
core temperature (Δ °C)
time to treatment (hr PI)
c
*
V_t (ml/breath)
Pre
Post (24h)
d
V_m (ml/min)
Pre
Post (24h)
DR61 (+12h)
DH27
IC70
IL40
JM39
EM61

Figure 3

A. Serum

	Control		4 hr intervention					12 hr intervention				
	DH27	JP56	LB98	IC70	IL40	LJ80	EM61	KP48	KR49	LB26	DR61	JM39
EGF	1.53	0.83	-0.17	0.73	0.28	-0.83	0.64	0.27	0.64	-0.67	0.79	1.42
Eotaxin	0.62	0.91	-0.01	0.48	0.31	0.28	0.40	-0.29	0.01	-0.05	-0.17	0.61
FGF-basic	0.38	1.49	0	0.33	-0.27	-0.32	0.40	0.25	0.28	-0.35	0.29	0.73
G-CSF	2.58	4.92	-0.07	0.05	-0.93	-0.22	-0.33	-0.14	-0.21	-0.33	-0.10	0.21
GM-CSF	1.58	2.16	-0.21	-0.05	0.08	-0.07	0.07	-0.03	0.04	-0.18	-0.07	0.26
HGF	0.33	0.68	-0.24	-0.10	-1.07	-0.22	0.04	-0.17	-0.16	-0.04	-0.15	0.23
IFN-g	0.53	0.74	-0.20	0.05	-1.15	-0.22	0	-0.13	-0.21	0	-0.24	0.57
IL-1b	0.99	1.56	-0.15	-0.01	-0.33	-0.06	0.15	-0.06	-0.03	-0.07	-0.38	0.44
IL-1RA	7.17	8.47	0.09	0.04	0.12	-0.47	1.73	1.68	0.84	1.55	1.35	3.74
IL-2	1.04	1.64	-0.08	-0.10	0.10	0	0.07	-0.07	0.07	-0.03	-0.21	0.13
IL-4	0.23	0.35	-0.15	-0.08	-0.58	-0.12	-0.11	0	-0.07	0.08	-0.14	-0.07
IL-5	1.04	1.95	-0.21	0.26	-0.97	-0.39	0.18	-0.06	0.15	-0.20	-0.38	0.06
IL-6	8.65	9.64	1.41	1.94	2.23	2.14	2.61	2.30	0.64	2.49	2.24	4.18
IL-8	-0.85	-1.52	-1.74	-1.87	-1.83	-2.01	-0.84	-2.28	-2.80	-1.78	-3.56	-1.90
IL-10	0.60	0.85	-0.06	-0.03	-0.77	-0.03	0.06	-0.01	0.10	0.05	0	0.12
IL-12	-0.44	0.05	-0.13	-0.27	-0.82	-0.43	0.07	-0.32	-0.25	-0.10	-0.22	-0.55
IL-15	0.57	0.96	-0.18	0.05	-0.61	-0.16	0.27	-0.08	0.02	-0.45	-0.11	0.21
IL-17	0.05	-0.08	-0.10	-0.12	-0.23	-0.40	0.04	-0.21	-0.18	-0.42	-0.18	0.14
I-TAC	-0.32	-0.17	-0.57	-0.74	0.50	-0.56	0.50	-0.19	-0.81	-0.71	-0.36	0.18
MCP-1	3.05	4.02	-0.16	0.73	0.72	0.28	1.68	-0.22	0.30	0.26	-0.31	1.41
MDC	-0.25	0.19	-0.16	-0.28	-0.04	0.17	0.33	0	0.23	0.08	-0.42	-0.36
MIF	2.00	1.74	0.27	1.09	0.22	-0.67	0.78	0.62	0.67	-0.48	1.39	0.86
MIG	0.31	0.38	-0.26	-0.18	-0.94	-0.07	-0.04	0.10	-0.18	-0.17	-0.20	0.25
MIP-1a	0.71	0.77	-0.16	0	-1.04	0.13	0.10	-0.15	0.17	0	-0.18	0.24
MIP-1b	0.44	0.82	-0.17	-0.04	-0.77	-0.20	0.08	-0.10	-0.10	0.14	-0.06	0.42
RANTES	0.04	0.08	-0.02	-0.03	-0.02	0.01	0.03	-0.04	-0.01	-0.06	-0.07	-0.01
TNF-a	0.30	0.58	-0.19	-0.02	-1.34	-0.11	0	-0.32	0.11	-0.21	-0.12	0.15
VEGF	3.18	3.71	0.32	0.31	1.16	0.14	0.67	0.73	0.20	0.67	0.44	1.57
IP-10	0.33	0.71	-0.10	-0.23	-1.12	-0.07	-0.10	-0.15	0	-0.17	-0.03	0.13

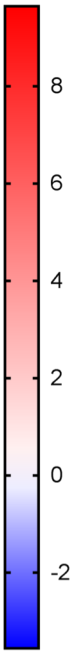

B. BAL

	Control	4 hr intervention					12 hr intervention				
	DH27	LB98	IC70	IL40	LJ80	EM61	KP48	KR49	LB26	DR61	JM39
EGF	0.10	0.07	0.12	0.26	-0.10	0.05	-0.02	0.19	0.22	0.22	0.29
Eotaxin	2.25	0.98	2.84	1.97	1.73	1.09	3.78	2.00	3.69	2.74	4.23
FGF-basic	0.62	0.41	0.13	0.14	-0.08	0.03	0.62	0.49	0.45	0.56	0.62
G-CSF	1.21	0.17	0.20	0.29	0.21	0.20	0.19	0.25	1.21	0.38	3.74
GM-CSF	1.02	0.26	0.50	0.64	0.80	0.57	1.00	1.23	1.29	1.11	1.65
HGF	0.21	0.09	0	0.29	0.13	0.05	0.42	0.37	0.52	0.23	1.02
IFN-g	-0.17	0.09	0.13	0	0.11	0	0.47	0.28	0.35	0.28	0.47
IL-1b	1.76	0.84	0.57	2.16	0.82	1.29	1.04	1.32	1.52	2.76	2.36
IL-1RA	2.28	0.10	0.98	2.09	1.10	1.52	2.25	2.81	1.75	3.72	3.41
IL-2	0.92	0.03	0.21	0.40	0.16	0.16	0.90	0.90	1.04	0.88	1.39
IL-4	0.22	0.15	0.08	0.03	0.12	0	0.35	0.14	0.22	0.29	0.51
IL-5	1.07	0.25	0.58	0.63	0.28	0.29	1.12	1.56	1.46	1.43	1.90
IL-6	6.25	3.79	5.20	5.40	4.16	4.53	6.79	5.27	7.74	7.96	7.79
IL-8	0.85	0.62	0.58	0.77	1.01	0.50	0.55	1.03	1.04	1.08	1.03
IL-10	0.08	0.04	0.08	0.06	0.03	0.01	0.27	0.73	0.34	0.23	0.53
IL-12	0.04	0.04	0.11	0.15	0.17	0.12	0.28	0.24	0.26	0.25	0.55
IL-15	-0.21	-0.02	0.09	0.16	-0.02	0.03	0.54	0.11	0.26	0.20	0.32
IL-17	0.20	0.07	0.17	0.58	0.16	0.03	0.74	0.69	1.52	0.22	0.69
I-TAC	-0.81	1.84	0.93	1.65	0.64	1.63	0.33	1.04	0.75	1.78	1.42
MCP-1	-0.89	2.69	2.02	3.02	3.78	3.51	3.83	3.71	5.19	1.97	4.65
MDC	-0.06	1.73	1.62	2.01	1.34	2.70	1.30	1.51	0.56	2.72	3.62
MIF	1.47	1.10	0.73	0.51	0.73	0.46	-0.48	1.11	0.07	-0.48	-0.86
MIG	0	0	-0.13	0.06	0.06	0.13	0.14	-0.21	0.16	0.29	0.20
MIP-1a	0.51	0.47	0.45	1.78	1.09	0.45	0.42	0.48	2.45	0.78	0.91
MIP-1b	0.64	0.06	0.13	0.27	0.13	0.07	0.72	0.49	1.42	0.46	0.81
RANTES	0.37	-0.22	-0.31	-0.39	-0.18	-0.09	-0.76	-0.08	-0.63	-0.58	-0.40
TNF-a	0.49	0.28	0.36	0.77	0.51	0.47	0.65	0.75	0.74	0.77	1.37
VEGF	-1.36	-0.24	0.50	-0.29	0.27	0.14	0.62	-0.30	1.34	2.02	0.39
IP-10	0.10	0.08	0.14	0.17	0.08	0.15	0.74	0.24	0.68	0.43	0.76

Supplemental Figures

Figure S1

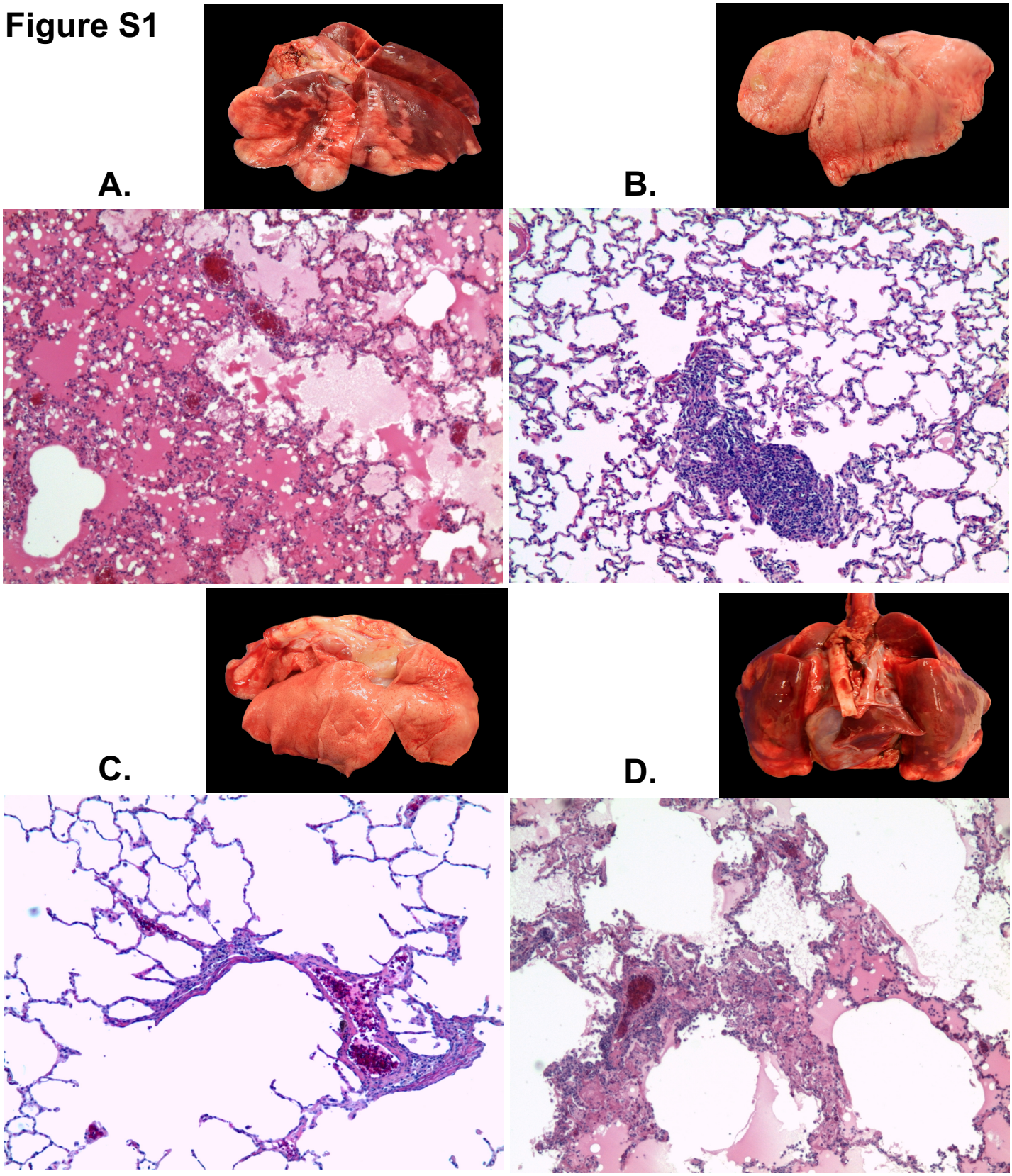

Figure S2

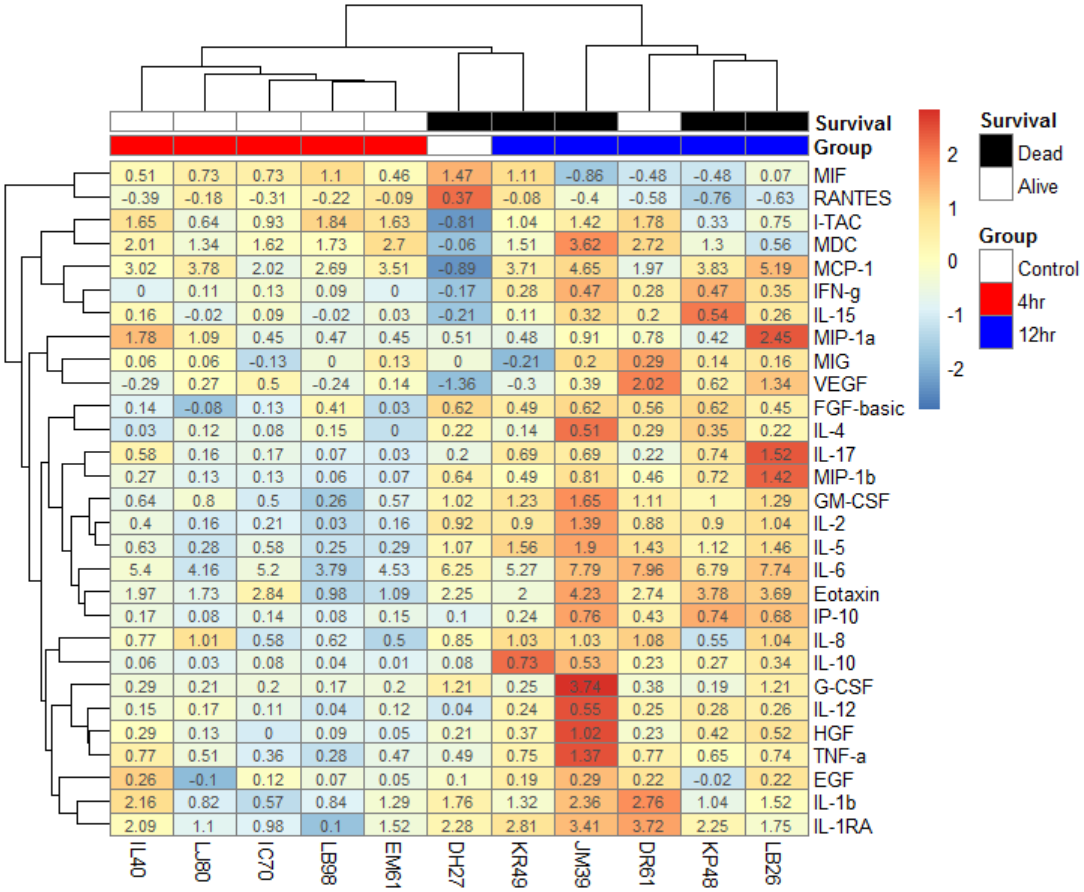
Survival
Group
MIF 0.51 0.73 0.73 1.1 0.46 1.47 1.11 -0.86 -0.48 -0.48 0.07
RANTES -0.39 -0.18 -0.31 -0.22 -0.09 0.37 -0.08 -0.4 -0.58 -0.76 -0.63
I-TAC 1.65 0.64 0.93 1.84 1.63 -0.81 1.04 1.42 1.78 0.33 0.75
MDC 2.01 1.34 1.62 1.73 2.7 -0.06 1.51 3.62 2.72 1.3 0.56
MCP-1 3.02 3.78 2.02 2.69 3.51 -0.89 3.71 4.65 1.97 3.83 5.19
IFN-g 0 0.11 0.13 0.09 0 -0.17 0.28 0.47 0.28 0.47 0.35
IL-15 0.16 -0.02 0.09 -0.02 0.03 -0.21 0.11 0.32 0.2 0.54 0.26
MIP-1a 1.78 1.09 0.45 0.47 0.45 0.51 0.48 0.91 0.78 0.42 2.45
MIG 0.06 0.06 -0.13 0 0.13 0 -0.21 0.2 0.29 0.14 0.16
VEGF -0.29 0.27 0.5 -0.24 0.14 -1.36 -0.3 0.39 2.02 0.62 1.34
FGF-basic 0.14 -0.08 0.13 0.41 0.03 0.62 0.49 0.62 0.56 0.62 0.45
IL-4 0.03 0.12 0.08 0.15 0 0.22 0.14 0.51 0.29 0.35 0.22
IL-17 0.58 0.16 0.17 0.07 0.03 0.2 0.69 0.69 0.22 0.74 1.52
MIP-1b 0.27 0.13 0.13 0.06 0.07 0.64 0.49 0.81 0.46 0.72 1.42
GM-CSF 0.64 0.8 0.5 0.26 0.57 1.02 1.23 1.65 1.11 1 1.29
IL-2 0.4 0.16 0.21 0.03 0.16 0.92 0.9 1.39 0.88 0.9 1.04
IL-5 0.63 0.28 0.58 0.25 0.29 1.07 1.56 1.9 1.43 1.12 1.46
IL-6 5.4 4.16 5.2 3.79 4.53 6.25 5.27 7.79 7.96 6.79 7.74
Eotaxin 1.97 1.73 2.84 0.98 1.09 2.25 2 4.23 2.74 3.78 3.69
IP-10 0.17 0.08 0.14 0.08 0.15 0.1 0.24 0.76 0.43 0.74 0.68
IL-8 0.77 1.01 0.58 0.62 0.5 0.85 1.03 1.03 1.08 0.55 1.04
IL-10 0.06 0.03 0.08 0.04 0.01 0.08 0.73 0.53 0.23 0.27 0.34
G-CSF 0.29 0.21 0.2 0.17 0.2 1.21 0.25 3.74 0.38 0.19 1.21
IL-12 0.15 0.17 0.11 0.04 0.12 0.04 0.24 0.55 0.25 0.28 0.26
HGF 0.29 0.13 0 0.09 0.05 0.21 0.37 1.02 0.23 0.42 0.52
TNF-a 0.77 0.51 0.36 0.28 0.47 0.49 0.75 1.37 0.77 0.65 0.74
EGF 0.26 -0.1 0.12 0.07 0.05 0.1 0.19 0.29 0.22 -0.02 0.22
IL-1b 2.16 0.82 0.57 0.84 1.29 1.76 1.32 2.36 2.76 1.04 1.52
IL-1RA 2.09 1.1 0.98 0.1 1.52 2.28 2.81 3.41 3.72 2.25 1.75
IL40 LJ80 IC70 LB98 EM61 DH27 KR49 JM39 DR61 KP48 LB26
2
1
0
-1
-2
Survival
Dead
Alive
Group
Control
4hr
12hr

Figure S3

Serum

BAL

A.

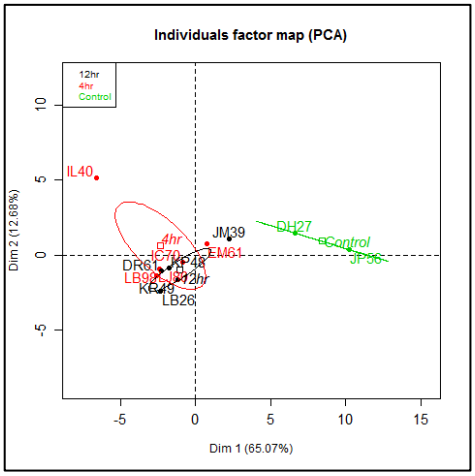

D.

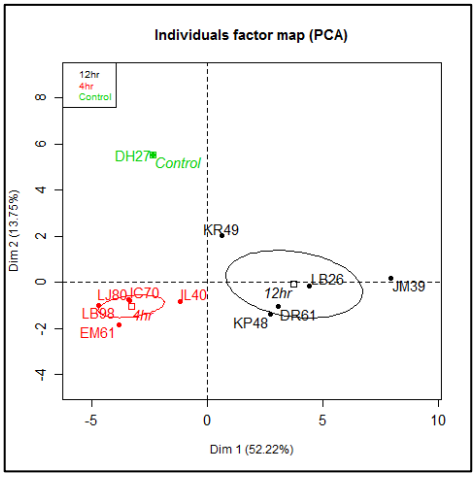

B.

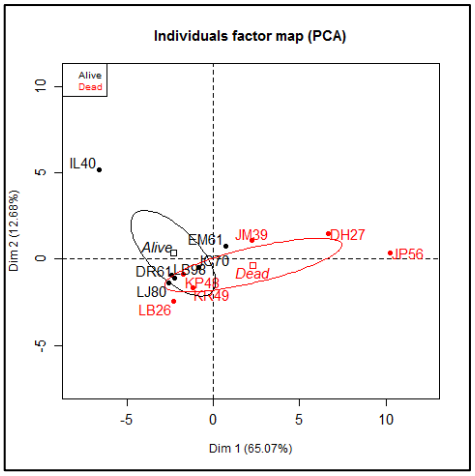

E.

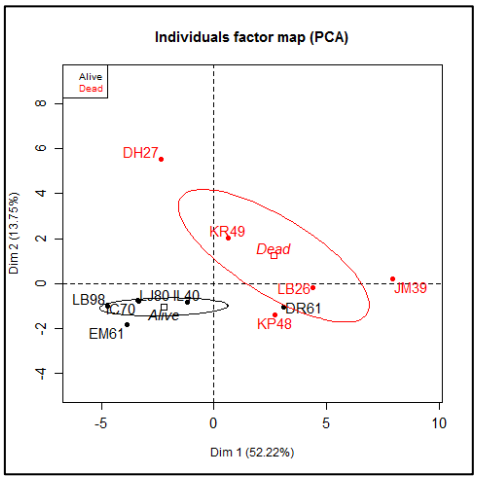

C.

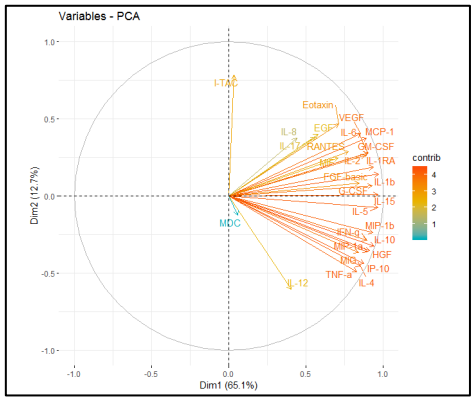
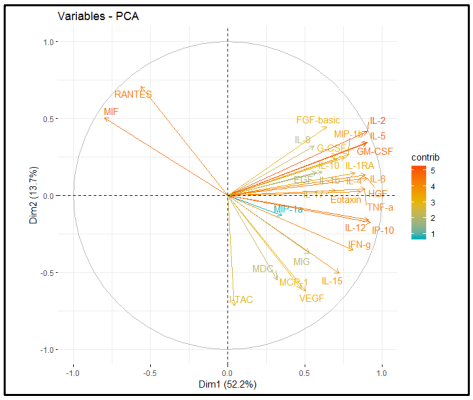
F.